ARCTIC
VOL. 44, SUPP. 1 (1991) P. 140-146

In Situ Measurements of Micro-Scale Surface Roughness of Sea Ice

J.S. PATERSON,[1] B. BRISCO,[1] S. ARGUS[2] and G. JONES[3]

(Received 6 June 1990; accepted in revised form 6 November 1990)

ABSTRACT. Surface roughness at the centimetre and millimetre scale is an important factor governing radar backscatter, especially in the case of warm (> −5°C) or highly saline sea ice types. Quantitative measurements of surface roughness are required as input to backscatter models. Several field techniques have been used to quantitatively measure the surface roughness of sea ice. These techniques usually possess at least one of the following obstacles: difficult field operation, expense, poor accuracies or arduous data processing.

A prototype portable field instrument called the Surface Roughness Meter has been designed to measure micro-scale surface roughness. The instrument provides measurements of two surface roughness parameters, root mean square height and correlation length. The instrument consists of a 35 mm camera and a flash mounted on a platform. The system illuminates and photographs a rectangle of known size on the surface from a fixed height. The negatives are digitized and the root mean square height and correlation length are calculated and recorded using a PC-based image analysis system in the laboratory.

The first sea ice application for the instrument was the Labrador Ice Margin EXperiment (LIMEX) 1989. The instrument was used to measure surface roughness of first-year deformed pack ice. The resulting data from LIMEX '89 were digitized and surface roughness statistics were computed using a PC image analysis system. LIMEX '89 Surface Roughness Meter data compared favourably to roughness statistics obtained from LIMEX '87.

Key words: surface roughness, radar backscatter, sea ice, Surface Roughness Meter, root mean square height, correlation length, LIMEX '89

RÉSUMÉ. La rugosité de la surface à l'échelle du centimètre et du millimètre est un facteur important dans la rétrodiffusion radar, surtout lorsqu'il s'agit de types de glace de mer tempérée (> à - 5°C) ou bien ayant un taux salin très élevé. Les modèles de rétrodiffusion nécessitent des données sur des mesures quantitatives de la rugosité de la surface. Il existe plusieurs techniques qui peuvent être employées sur le terrain pour mesurer quantitativement la rugosité de la surface de la glace de mer, et ces techniques comportent généralement au moins un des inconvénients suivants: difficulté des opérations sur le terrain, coût, faible précision ou traitement laborieux des données.

Pour mesurer la rugosité de la surface à une micro-échelle, on a conçu un prototype d'instrument portable, appelé profilographe, qu'on utilise sur le terrain. Cet instrument fournit des mesures de deux paramètres de la rugosité de la surface, soit la hauteur quadratique moyenne et la longueur de corrélation. L'instrument consiste en un appareil photo de 35 mm et un flash monté sur une plate-forme. Un rectangle de la surface dont les dimensions sont connues est illuminé et photographié à partir d'une hauteur fixe. Les négatifs sont numérisés et la hauteur quadratique moyenne ainsi que la longueur de corrélation sont calculées et enregistrées dans le laboratoire à l'aide d'un système d'analyse d'images utilisant un micro-ordinateur.

La première application de cet instrument à la glace de mer a eu lieu en 1989, dans le cadre de l'Étude de la zone marginale des glaces du Labrador (LIMEX). On a utilisé alors le profilographe pour mesurer la rugosité de la surface de la glace de banquise déformée de première année. Les données qui ont résulté de cette étude ont été numérisées et on a employé un système d'analyse d'images utilisant un micro-ordinateur pour calculer les statistiques concernant la rugosité de la surface. Les données du profilographe utilisé dans le cadre de LIMEX '89 se sont comparées favorablement aux statistiques sur la rugosité, obtenues au cours de l'expérience LIMEX '87.

Mots clés: rugosité de la surface, rétrodiffusion radar, glace de mer, profilographe, hauteur quadratique moyenne, longueur de corrélation, LIMEX '89

Traduit pour le journal par Nésida Loyer.

INTRODUCTION

The monitoring of sea ice in Canada is of great importance to oil and mineral exploration, the coast guard, commercial shipping and global change climatological studies. Sea ice is a dynamic material consisting of floes of varying thickness and composition, which can change both temporally and spatially. Due to persistent cloud cover and darkness over Canada's ice-infested waters, optical-type sensors are inappropriate for monitoring sea ice. Since Synthetic Aperture Radar (SAR) sensors can take images regardless of darkness or cloud cover, SAR will undoubtedly play a key role in sea ice monitoring in the future.

The potential to use imaging SAR for monitoring earth resources on a routine basis will soon become a reality with the approaching launches of European Space Agency Earth-Resources Satellite (E-ERS-1), Japanese Earth Resources Satellite (J-ERS-1), the Canadian Radarsat and the Earth Observation Satellite (EOS). Although a great wealth of data will be provided by these satellites, effective methods for utilizing SAR data will not be fully exploited until the link between the real and the imaged world is better established. This requires knowledge of the interaction of microwaves with the surface and determination of properties that govern the amount of radiation reflected back to the sensor (backscatter). Establishing this relationship is a complex task owing to the spatial and temporal variability of the sea ice. Once the interaction is understood, it will be possible to derive geophysical properties of sea ice from SAR data.

The portion of emitted microwave energy returned to a sensor is a function of the scattering mechanisms at the surface, which in turn are a function of the surface dielectrics (the reflectivity and conductivity of a material) and roughness and the angle of incident energy. Establishing the link between surface and subsurface properties and microwave response requires quantitative measurement of the various surface and subsurface parameters that affect backscatter. Quantitative surface measurements can be related to SAR backscatter through the use of backscatter models (Livingstone and Drinkwater, in press; Ulaby *et al.*, 1982). The ultimate goal of these models is inversion, which enables extraction of ice information from SAR data. Most surface scattering theories include root mean square (rms) and correlation length parameters for surface geometry definition (Ulaby *et al.*,

[1]Intera Kenting Limited, 2 Gurdwara Road, Suite 200, Nepean, Ontario, Canada K2E 1A2
[2]Canada Centre for Remote Sensing, 2464 Sheffield Road, Ottawa, Ontario, Canada K1A 0Y7
[3]Richard Brancker Research Ltd., 27 Monk Street, Ottawa, Ontario, Canada K1S 3Y7

1982). Work is in progress to ensure that the process of extracting ice information will be automated and/or sampled, with the result that the large volumes of satellite data can be utilized (Hirose and McNutt, 1988).

Properties governing backscatter include micro- and macro-scale roughness, dielectrics, surface wetness, density and bubble size and spacing, grain size and salinity (Winebrenner *et al.*, 1989). One of the most important factors governing SAR backscatter from a surface is the micro-scale roughness of the surface. Surface roughness becomes increasingly important with increasing sea ice salinity and with increasing free water content in the snow cover (Drinkwater, 1988; Stiles and Ulaby, 1980; Ulaby *et al.*, 1984).

The development of suitable instruments that provide accurate and quantitative results suitable for model ingestion has occurred relatively recently (Drinkwater, 1989; Livingstone and Drinkwater, in press). A new instrument developed by Richard Brancker Research Ltd. and the Canada Centre for Remote Sensing (CCRS) Agriculture Applications Group has been tested in the Canadian east coast marginal ice zone, in several soil applications experiments and as part of a laboratory program, Cold Regions Research and Engineering Laboratory EXperiment '89/90 (CRRELEX). The type of data from this instrument has been shown to be of use in modelling SAR response (Livingstone and Drinkwater, in press).

BACKGROUND

Surface Roughness

Micro-scale surface roughness is defined as the millimetre and centimetre scale changes or irregularities in vertical relief of a target surface (Sabins, 1986). Surfaces with roughness changes > 100 or 150 mm are considered to be very rough surfaces at C-band SAR wavelengths and may be considered as macro-scale roughness features. Such features include ridges, rubble, floe edges and rafted floes. This paper deals with the measurement of the micro-scale surface roughness rather than macro-scale roughness.

Smooth surfaces produce a dark signature on an SAR image caused by specular reflection, where all the incident energy is reflected and does not return to the sensor. In contrast, slightly rough surfaces will produce brighter regions on a SAR image as a portion of the energy is scattered and returned to the sensor. In the case of very rough surfaces, of the order of several centimetres, surface scattering is dominated by diffuse scattering. The transition between specular and diffuse scattering as a function of the surface is shown in Figure 1 (after Ulaby *et al.*, 1982).

The Fraunhofer criterion can be used for the purpose of modelling the scattering of surfaces in the microwave region when the wavelength is in the order of the standard deviation of the surface height (Ulaby *et al.*, 1982). The Fraunhofer criterion can be applied to consider if a surface is electromagnetically "smooth." If the combination of the roughness scale and wavelength is below a certain limit, then the criterion may be filled and a surface may be described as smooth. In order for the Fraunhofer criterion to be applied, the SAR wavelength must be on the order of the mean surface standard deviation height (σ_h) (Ulaby *et al.*, 1982). The CCRS C-band SAR fulfills the Fraunhofer criterion for sea ice surfaces, and therefore a smooth surface to the CCRS C-band radar can be defined by the following: Fraunhofer criterion $\sigma_h < \frac{\lambda}{32 \cos \theta}$, where σ_h = standard deviation of height, λ = radar wavelength and θ = radar incidence angle.

The CCRS C-band radar has a wavelength of 56.6 mm and the incidence angle is between 45° and 75° in narrow swath mode (Livingstone *et al.*, 1987). Therefore, solving the Fraunhofer equation for the C-band CCRS SAR system, a surface will appear smooth if the standard deviation (σ) is < 2.5 mm at 45° incident angle (near range) and < 6.8 mm at 75° incident angle (far range). It should be noted that a surface at C-band that appears "rough" could appear smooth at L-band due to the longer L-band wavelength of 235 mm as compared to C-band's 56.6 mm wavelength.

The derivation of σ_h and the surface correlation length (ℓ) are computed in the same manner as described by Ulaby *et al.* (1982). The ice surface is assumed to be a random surface, without periodicity. σ_h and ℓ describe the statistical variation

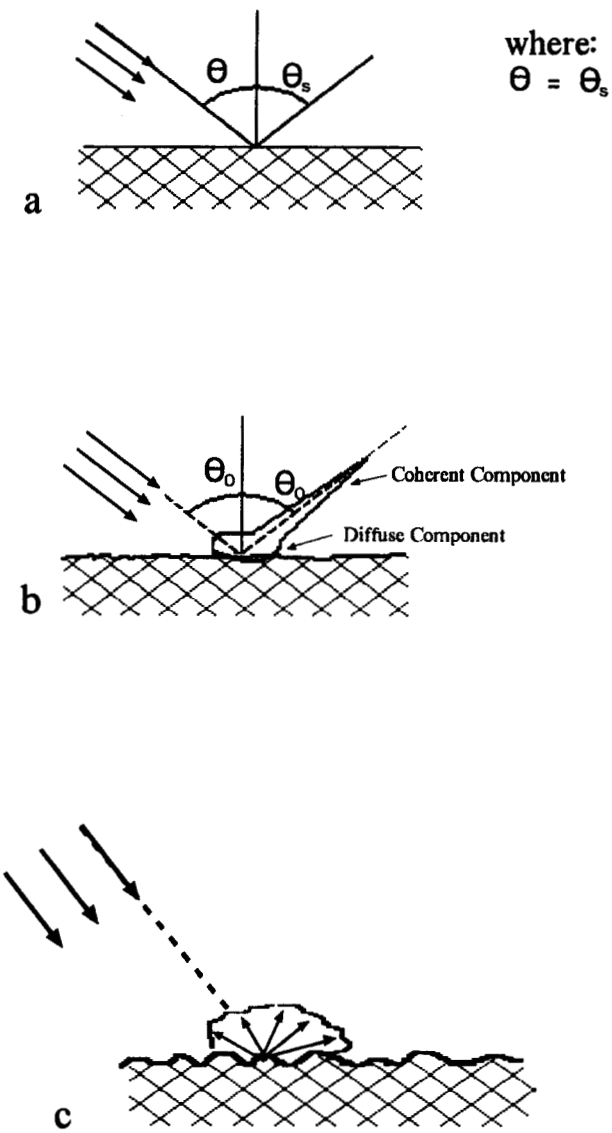

FIG. 1. SAR scattering, showing relative contributions of coherent and diffuse scattering for a) perfectly smooth specular surface, specular reflection results; b) slightly rough surface, large, coherent component and small, diffuse non-coherent component; and c) rough surface — scattering pattern is diffuse, near isotropic (after Ulaby *et al.*, 1982).

of the random component of the surface height relative to a zero mean reference surface (Ulaby *et al.*, 1982). Since the ice surface is assumed to be non-periodic, the rms height is the same as σ_h. The normalized autocorrelation function is a measure of similarity between height z at a point x and point x′ at a distance from x, where $x' = (j-1)\,\Delta x$, with Δx as the spatial sampling interval in the horizontal direction and the lag value j is an integer ≥ 1 (Ulaby *et al.*, 1982). The statistical independence of sampling points on a surface can be estimated using ℓ. The surface correlation length is derived from the normalized autocorrelation function and is defined as the displacement x′, where $p(x')=1/e$ ($\approx .37$) (Ulaby *et al.*, 1982). With non-specular surfaces, if two points on the surface are separated by a horizontal distance greater than ℓ, their heights may be considered to be statistically independent of one another (Ulaby *et al.*, 1982).

Instrumentation

Although several techniques and instruments have been used to measure surface roughness for the purpose of radar backscatter modelling and for soil erosion studies, an accurate and economic solution has yet to be discovered. The most primitive method for measuring roughness is with a ruler and the human eye. Understandably, the ruler/eyeball method is prone to considerable error and it is difficult to obtain a representative sample. Instruments used to measure surface roughness are generally either the mechanical or optical type. Mechanical surface roughness instruments are referred to as profile or rill meters, and in the past they have been the most commonly used field instruments. The profile meter resembles an oversized comb consisting of approximately 100 freely moving metal rods or pins held together by a bracket. The rods are free to descend to the surface and characterize the surface micro-relief. After the rods are lowered, a black board is held behind the top of the pins for contrast and a black and white photograph is taken of the pin displacement, as shown in Figure 2. The photographs are digitized in the laboratory and σ_h and ℓ are computed. Typical instruments of this kind have a sampling interval of approximately 10 mm, a range of up to 900 mm and a sample size of about 1000 mm. Several shortcomings are associated with such profiling instruments. Profiling meters are awkward to use, require two persons to operate and, depending on the conditions of the surface, the surface roughness elements can be destroyed on contact with the rods so measurements are not representative of the actual roughness. Mechanical profile meters have been used by Hirschi *et al.* (1987), Moore and Larson (1979), McCool *et al.* (1981) and Drinkwater (1989).

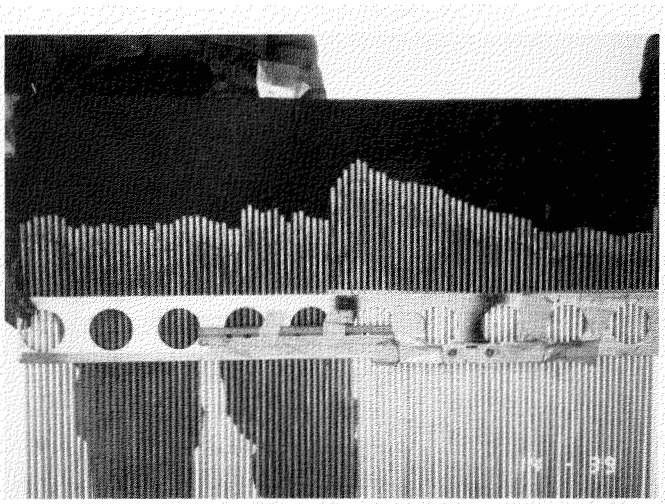

FIG. 2. JPL Profilometer (Drinkwater, 1989) application during LIMEX '87. Photograph courtesy of B. Holt (JPL).

Optical methods for measuring surface roughness are more desirable since the instrument does not disturb the target surface, the vertical and horizontal resolution is greater and potentially higher accuracies may be achieved. Römkens *et al.* (1988) describe an optical laser micro-reliefmeter with maximum accuracies in the vertical and horizontal surface of 0.25 mm and 0.001 mm respectively and a sample measurement surface of 2.6 m. Laser optical surface roughness instruments are accurate, but they can also be very expensive and can be difficult to transport, set up and operate in the field.

In response to the need for a portable, accurate and economical field instrument to provide measurements of micro-scale surface roughness of ice, snow and soils for SAR backscatter modelling, CCRS and Richard Brancker Limited have funded and designed a prototype instrument called the Surface Roughness Meter (SRM).

INSTRUMENT DESCRIPTION

The design requirement was to build an optical instrument for rapid, cost-effective, non-destructive, reliable and accurate *in situ* field measurements of surface roughness parameters. The approach is similar to that described by Yoshizawa *et al.* (1987). This technique uses the illumination of a rectangle of known dimension onto the surface with simultaneous high-contrast black and white film capture using a 35 mm camera. Post-processing and analysis of the film in the laboratory produces the roughness statistics, σ_h and ℓ.

Two different surface roughness instrument designs have been built. The first instrument was built in 1988 and was tested during both sea ice and agriculture field experiments in 1988-89. The second SRM prototype was an improved system based on the experiences from these CCRS field applications in 1988-89. Both instruments have the same concept and geometric configuration; differences between the two prototypes lie in the instrument platform. The first SRM consists of a bar with a 35 mm Nikon camera and flash mounted on a camera tripod (Fig. 3). Due to the instability of this instrument an updated version possessing a robust and fully stable three-legged bench-like platform was designed (Fig. 4). A technical description of the first SRM prototype is provided by Brisco *et al.* (1989). A black sun shroud fits around the instrument, inhibiting ambient light from entering the measurement area and ensuring good contrast between the illuminated rectangle and the surrounding area. The camera is mounted at an angle of 20° relative to the flash; the angle can be adjusted to alter the range and resolution. The SRM must be levelled by adjusting the leg height and monitoring the level bubbles on the instrument. The SRM illuminates and photographs a 550 mm × 130 mm rectangle on the surface from a height of 1200 mm. Figure 5 illustrates the geometry of the field component of the surface roughness instrument.

Post-experiment analysis consists of digitizing the negatives and extracting σ_h and ℓ by computerized methods. The exposed negatives are analyzed using a PC-based image

FIG. 3. First surface roughness meter (SRM) prototype. The original design consisted of a camera tripod as its support base, which was found to be inappropriate for field use.

analysis work station. The work station consists of an IBM compatible computer, a specialized analysis software package, a Matrox PIP-512 video digitizing card and a small television monitor. Using the SRM work station, negatives are digitized and σ_h and ℓ values are calculated along both edges of the illuminated rectangle. Analysis of the edge is done using the (x, y, z) coordinates for each point on the digitized grid edge. The following equations taken from Brisco *et al.* (1989) define each of the coordinates: $x = (h-z) \tan(\phi)$; $y = y(tv)(h-z)/(\cos(\alpha) - x(tv) \sin\alpha)$; $z = h - d/(\tan(\phi) - \tan(\phi))$; where: h = projector to reference plane distance; d = camera to projector distance; $\alpha = \arctan(d/h)$; $\Theta = \alpha + \arctan(x(tv))$; $\phi = \arctan(x(t)/h)$; and: x(tv) = measured coordinates from TV image; y(tv) = measured coordinates from TV image; x(t) = true x position of edge.

The roughness analysis software provides the user with several options for processing the data, such as to plot the rms height and autocorrelation function of the sample, produce an ASCII format file, which can be exported to a statistical or graphical package for further analysis, and calibration of the system geometry. The analysis software uses the correlation length computation given by Ulaby *et al.* (1982). The autocorrelation function is computed for the vertical height z and the correlation length ℓ, where $\ell = 1/e$ (Ulaby *et al.*, 1982).

The video and digitizing processes are the limiting factors associated with resolution. The Matrox video consists of 512 × 512 pixels (picture elements), yielding a resolution of about 1 mm in the horizontal (y) direction, since the SRM sample length (illuminated rectangle) is approximately 550 mm. For the vertical resolution (z), the resolution is about ±4 mm, since the 20° angle separating the camera and the flash is also a limiting factor. The maximum vertical height of a target on the surface is approximately 300 mm and the error for the process is ±4.0 mm. There is a trade-off between system resolution and height of the camera above the measurement surface. The trade-off is that as the height of the camera above the surface increases, the resolution of the system decreases, but the sample size (size of the rectangle projected on the surface) increases.

Verification of calibration and resolution of the instrument has been performed by Brisco *et al.* (1989). Pieces of wood of known dimensions were imaged using the SRM, and σ_h and ℓ were computed. Results from the calibration yielded

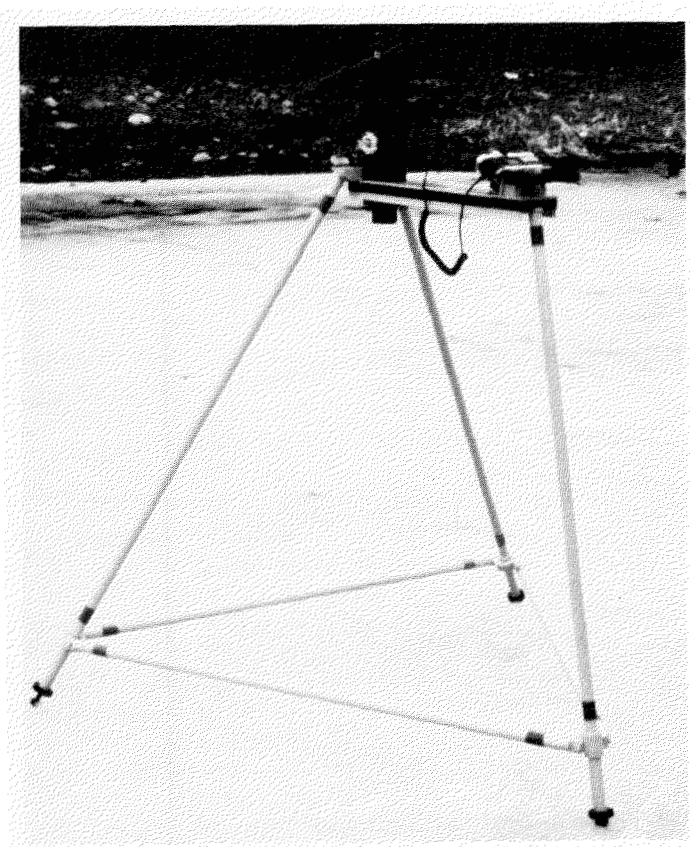

FIG. 4. Second surface roughness meter (SRM) prototype without the sun shroud. The new support base corrected the problems encountered during LIMEX '89 operation.

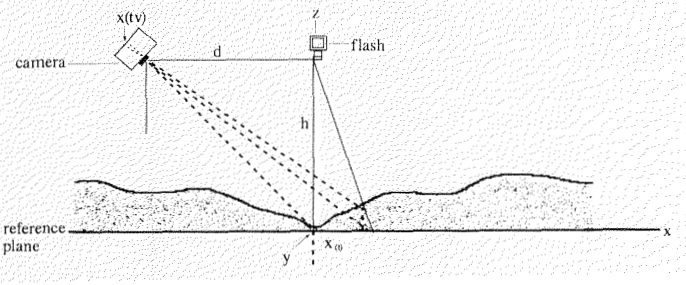

FIG. 5. Geometry of the SRM field instrument (after Brisco *et al.*, 1989).

a standard deviation of 4.19 mm for the height (z) and 2.66 mm for the width (y). Low contrast between the wood targets and the carpet background presumably gave rise to a slightly higher standard deviation.

Recent analysis of artificial surfaces with known rms height and correlation length produced accuracies of 2 mm in z, which surpass the resolution of the system. This is attributed to statistical averaging. The SRM is still considered as a prototype instrument and work is continuing to improve the accuracy of the system. A future improvement to the digitizing process is the addition of two cylindrical lenses between the negative and television camera. This future hardware addition should increase the z resolution by a factor of 4 to achieve a system resolution of 1 mm (x) by 1 mm (z).

Calibration of the system is recommended prior to collecting a data set. A flat surface, such as a floor or a piece of plywood, is imaged using the standard default instrument settings, and the size of the illuminated rectangle on the surface is recorded. The SRM software allows the user to calibrate the system using these measurements to compute the required scale factors from the video image.

FIELD TRIALS

LIMEX '89 (Labrador Ice Margin EXperiment '89) was the second in a series of Canadian-led international experiments to study the Labrador Sea marginal ice zone during the time of maximum sea ice extent. The objectives of LIMEX are to quantify the extent to which microwave, remotely sensed data are able to yield information on the status and evolution of the physical environment, to support operational methods for monitoring and forecasting events of significance, and to quantify ice and ocean characteristics in this region (Argus, 1989). A ship-based field program occurred during March 1989 with various sea ice physical properties collected in support of airborne SAR and shipborne radar and passive microwave measurements.

The first SRM prototype was field tested during LIMEX '89. During the experiment approximately 110 images were acquired from five locations off the Newfoundland coast on five days, 9, 10, 11, 12 and 17 March. Also collected on four of the five days were CCRS CV-580 airborne C- and X-band SAR data. On the first two sampling days, 9 and 10 March, the instrument was used in the morning during daylight hours. Due to strong winds the shroud billowed into the photographic sample area. The resulting samples either had a poorly defined rectangle due to light contamination or the shroud was imaged. To circumvent the problem of the light leakage, the remainder of the surface roughness data were obtained after sunset without the shroud.

The ice surface temperatures sampled with the SRM were relatively warm, ranging from -11 to -1°C, while surface salinity was relatively high, fluctuating from 13 ppt to 17.5 ppt, and bulk mean ice core salinity ranged between 4 and 9 ppt. The high salinity of the sea ice coupled with the relatively warm ice surface temperatures should inhibit C- and X-band microwave penetration, and therefore surface scattering should result (Drinkwater, 1989).

Pack ice concentrations were 9/10, consisting of mostly medium to thin first-year ice types, with floes of diameter <20 m. Approximately 10% of the ice consisted of brash, a slush-like ice mixture between floes. Pressure-induced ice rafting was evident throughout LIMEX '89, with severe rafting occurring prior to 11 March. Rafting caused ice floes to be tilted, and in some cases floes were subducted and stacked on top of each other, a micro-scale analogy to what occurs at active tectonic zones. Rafting is also responsible for the development of small levees of up to 500 mm in height and the formation of the interstitial brash ice.

The SRM sampling strategy employed during LIMEX was to start data collection approximately in the centre of a floe and move across the floe to the adjacent floe, collecting data about every metre. Dry snow was delicately swept away from the ice surface before SRM data was collected, since C- and X-band microwave energy should transmit directly to the ice surface without scattering in the dry snow layer (Ulaby *et al.*, 1984). A variety of surface roughness was encountered using this technique, including flat ice surfaces, ice nodules, small ice chunks, small ridges, ice floe edges and brash ice.

Approximately 25% of the 110 samples had to be discarded due to the scale of floe edges and levees — amplitudes of over 300 mm, which is out of the SRM range of measurement. Figure 6 illustrates an SRM sample of a floe edge that could not be accurately digitized due to the 500 mm relief change of a tilted floe edge. Data was lost on one day due to a photographic contrast problem when sampling clear ice.

Figure 7 displays two contrasting surface roughness images from LIMEX '89. Note the differences between an undeformed, relatively flat floe surface with $\sigma_h = 7.8$ mm (Fig. 7a) and a rough edge of a deformed sea ice floe with $\sigma_h = 52.6$ mm (Fig. 7b). Surface roughness > 200 mm in the marginal ice zone is the result of rafted floes and rubble ice (Fig. 8) and cannot be measured with this instrument.

The average σ_h value computed for LIMEX '89 using the SRM was 26.4 mm. The average σ_h value computed for LIMEX '87 data of similar ice using the Jet Propulsion Laboratory (JPL) profiling meter was comparable at 27.2 mm (Drinkwater, 1989). The σ_h value for relatively flat, undeformed sea ice using the SRM during LIMEX '89 was found to be 15.2 mm, whereas during LIMEX '87, profile

FIG. 6. SRM image of a tilted floe edge illustrating the difficulty of digitizing extreme changes in surface relief.

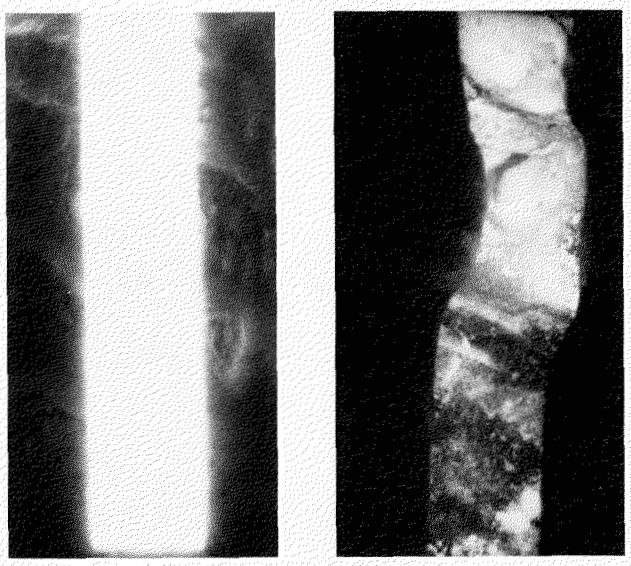

FIG. 7. LIMEX '89 SRM images showing examples of smooth sea ice and rough sea ice. 7a shows SRM images of relatively smooth, undeformed sea ice with an rms of 7.8 mm. 7b shows SRM images of rough sea ice from LIMEX '89 with an rms of 52.6 mm.

FIG. 8. Rough sea ice LIMEX '89 — deformation in the pack gave rise to rafted floes and ice rubble that were typically > 300 mm in amplitude.

meter average rms for flat, undeformed sea ice was 17.4 mm (Drinkwater, 1989). The higher σ_h value for LIMEX '87 data can be attributed to the degree of ice deformation between '87 and '89 on the east coast of Canada. In '87 the east coast ice underwent extreme compression in a westerly direction, forcing the pack ice against the coast, whereas in '89 a dominant westerly wind carried the pack ice 100 km offshore (Carsey *et al.*, 1988). After 16 March this difference is attributable to a melt and refreezing event during LIMEX '89 that created a smooth ice surface. Therefore, the values of σ_h obtained for the Labrador sea ice indicate that such sea ice will appear rough to a C-band SAR, as compared to a calm ocean surface using the Fraunhofer criterion.

Several major SRM design flaws were discovered during data collection over the LIMEX '89 field program. The sun shroud was found to be impossible to use even in light winds. The tripod used was unstable, cumbersome and difficult to adjust and the legs flexed under the weight of the equipment, altering the height of the camera. The screw mechanism holding the arm on which the camera is attached constantly loosened. A locking mechanism is needed to properly hold the arm in place. Lastly, the flash unit was not securely mounted for field use. All these instrument hardware design problems have been rectified with the design of the new SRM prototype (Fig. 4). The new prototype has a stable platform, the camera and flash are securely attached and it is now easier to assemble and use than its predecessor.

During LIMEX '89 field work, a photographic contrast problem was discovered when sampling clear ice, which rendered the data difficult to digitize. The problem arises when light diffuses through the ice so the line between illuminated and non-illuminated ice is not focused. The clear ice contrast problem resulted from the addition of water to the ice surface due to snow melt and a rainstorm, followed by cold temperatures causing freezing of surface water producing a smooth, clear ice surface. The clear ice problem also occurred with artificially grown sea ice during CRRELEX '89/90.

In order to find a solution to the clear ice problem an experiment was conducted to test various camera filters (yellow, orange, red, blue, .6 neutral density and UV filters), a range of camera f-stops and a technique to alter the surface contrast by applying a sprinkling of blue chalk dust. The site selected for the experiment was under a bridge on the frozen Rideau Canal in Ottawa, Ontario, during winter. Under the bridge ice growth resulted from a calm environment, shielded from snow accumulation. The resulting ice was smooth and clear, perfect for testing the SRM photographic contrast problem. Two smooth test sites and an artificially roughened surface were selected under the bridge. SRM data were collected at all three sites using all filters, a range of f-stops and an application of blue chalk dust.

Results indicated that the coloured filters, the neutral density filter and the UV filter had a negligible effect upon the contrast in the photograph. Altering the camera f-stops also had a very small effect on the edge contrast of the clear ice photograph, although large apertures reduce the problem somewhat. The application of blue chalk dust provided an excellent photographic contrast.

A thin millimetre dusting of chalk dust was manually sprinkled on the ice surface. Although it was difficult to apply a perfectly even distribution of chalk dust manually, care was taken administering the dust to ensure an even coverage to the ice surface. SRM data was collected immediately after the application of chalk dust, therefore limiting the chance of the chalk dust chemically altering the ice surface. It was found that even a sparse dusting on the part of the SRM sample region altered the contrast of the exposure to enable a clear edge to digitize. Figure 9 illustrates the marked difference between an SRM photograph of a clear ice surface with and without the blue chalk dust. The resulting photographs were easily and accurately digitized. A major drawback of using the chalk dust operationally is that the dust alters the ice surface. Small depressions may be filled in or a heavy dusting can cause micro-scale ridges, which alter the natural roughness of the ice surface. Also the addition of chalk to the ice surface is not recommended in environmentally sensitive areas such as the Arctic. Therefore the authors are not recommending the application of chalk

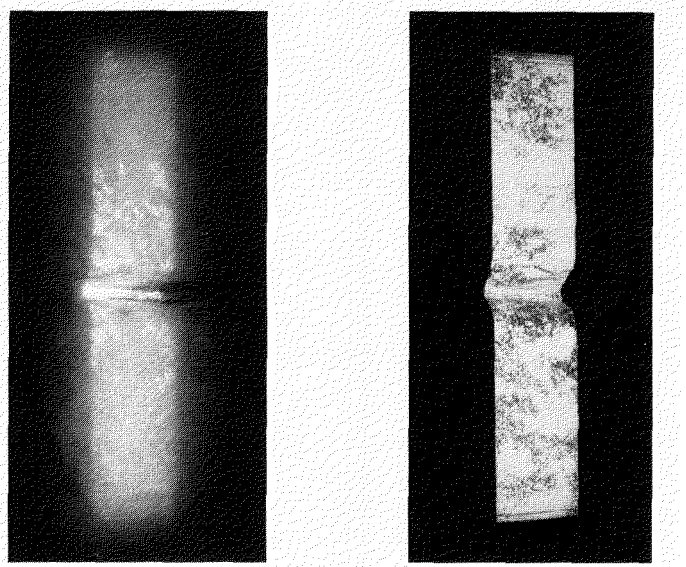

FIG. 9. Clear ice contrast problem — 9a shows an SRM photograph of clear ice without altering the surface, and 9b shows the marked difference in contrast in the photo of the same surface when blue chalk dust is applied.

dust to solve the clear ice problem, and other photographic methods for improving the contrast are being pursued.

CONCLUSION

The SRM is currently undergoing calibration using machined surfaces of known rms and correlation length. This calibration should provide a better measure of the system's accuracy. Enhancements to the SRM image analysis software are ongoing.

The second version of the SRM was field tested by the CCRS Agriculture group during SAR experiments in the spring and summer of 1990. Roughness statistics derived from this field work are currently being used in SAR modelling work. Agricultural field work with the SRM has shown the field portion of the SRM to be field-worthy, and therefore no design modifications of the field portion of the SRM are envisioned for the future.

The first prototype SRM was used to collect sea ice surface roughness measurements over the duration of the Sea Ice Monitoring Site (SIMS) experiment held in the Resolute Bay area during spring 1990. Although a large data set was collected over the four-week span of the experiment, about 50% of the data was discarded due to light penetration of the sample region and a camera failure. SIMS SRM data will be used in a study of physical changes in ice and snow during melt as related to SAR backscatter.

Future field work is planned for the second version of the SRM prototype during SIMS '91. A comparison study of sea ice roughness using the SRM and a laser profiling system is planned for SIMS '91.

ACKNOWLEDGEMENTS

Especial thanks go to the Canada Centre for Remote Sensing (CCRS) Agriculture Applications Group for the loan of the Surface Roughness Meter for LIMEX '89. The CCRS Ice Applications Group is very grateful for the technical guidance and inspiration given by B. Brisco, from the CCRS Agricultural Group. We would also like to thank the Radar Data Development Program for funding the field work. Other funding and the engineering of the instrument was performed by Richard Brancker Research Limited of Ottawa, Ontario. The authors would like to thank M. Drinkwater, of JPL, for constructive criticism of the paper.

REFERENCES

ARGUS, S. 1989. LIMEX '89 operations manual. Unpubl. ms. Available at the Canada Centre for Remote Sensing, 2464 Sheffield Road, Ottawa, Ontario, Canada K1A 0Y7.

BRISCO, B., BROWN, R.J., CIHLAR, J., and BRANCKER, R.W.S. 1989. A field instrument for surface roughness measurement. International Geoscience and Remote Sensing Symposium '89, Vancouver, B.C., 9-13 July. 1117-1180.

CARSEY, F.D., and DIGBY-ARGUS, S. 1988. Use of SAR imagery and other remotely-sensed data in deriving ice information during a severe ice event on the Grand Banks. International Geoscience and Remote Sensing Symposium '88, Edinburgh, Scotland, 12-16 September. 1431-1434.

CARSEY, F.D., DIGBY-ARGUS, S., COLLINS, M.J., HOLT, B., LIVINGSTONE, C.E., and TANG, C.L. 1988. Overview of LIMEX '87 ice observations. Institute of Electrical and Electronics Engineers Transactions on Geoscience and Remote Sensing 27(5):468-481.

DRINKWATER, M.R. 1988. Radar altimetric studies of polar ice. Ph.D. thesis, University of Cambridge, Cambridge, England.

———. 1989. LIMEX '87 ice surface characteristics: Implications for C-band SAR backscatter signatures. Institute of Electrical and Electronics Engineers Transactions on Geoscience and Remote Sensing 27(5):501-513.

HIROSE, T.K., and McNUTT, L. 1988. Toward an automated sea ice motion tracker. Unpubl. report. Available from the Canada Centre for Remote Sensing, 2464 Sheffield Road, Ottawa, Ontario, Canada K1A 0Y7.

HIRSCHI, M.C., BARFIELD, B.J., MOORE, I.D., and COLLIVER, D.G. 1987. Rill meters for detailed measurement of soil surface heights. Applied Engineering in Agriculture 3(1):47-51.

LIVINGSTONE, C.E., and DRINKWATER, M.R. In press. Spring time C-band SAR backscatter signatures of Labrador Sea marginal ice: Measurements vs modelling predictions. Institute of Electrical and Electronics Engineers Transactions on Geoscience and Remote Sensing.

LIVINGSTONE, C.E., GRAY, A.L., HAWKINS, R.K., OLSEN, R.B., and HALBERTSMA, J.G. 1987. CCRS C-band airborne radar-system description and test results. Paper presented at the 11th Canadian Symposium on Remote Sensing, Waterloo, Ontario, 22-25 June.

McCOOL, D.K., DOSSETT, M.G., and YECHA, S.J. 1981. A portable rill meter for field measurements of soil loss. Proceeding of the International Symposium, June 1981, Florence, Italy. 560-566.

MOORE, I.D., and LARSON, C.L. 1979. Estimating micro-relief surface storage from point data. Transactions of the American Society of Agricultural Engineers 22(3):663-669.

RÖMKENS, M.J.M., WANG, J.Y., and DARDEN, R.W. 1988. A laser microreliefmeter. Transactions of the American Society of Agricultural Engineers 31(2):408-413.

SABINS, F.A. 1986. Remote Sensing Principles and Interpretation. 2nd ed. New York: W.H. Freeman and Company.

STILES, W.H., and ULABY, F.T. 1980. The active and passive microwave response to snow parameters: 1. Wetness. Journal of Geophysical Research 85(C2):1037-1044.

ULABY, F.T., MOORE, R.K., and FUND, A.K. 1982. Microwave Remote Sensing Active and Passive. Vol. 2. Reading, MA: Addison-Wesley. 457-1064.

ULABY, F.T., STILES, W.H., and ABDELRAZIK, M. 1984. Snowcover influence on backscattering from terrain. Institute of Electrical and Electronics Engineers Transactions on Geoscience and Remote Sensing GE-22(2):126-132.

WINEBRENNER, D., TSANG, L., WEN, B., and WEST, R. 1989. Sea ice characterisation measurements needed for testing of microwave remote sensing models. Institute of Electrical and Electronics Engineers Journal of Oceanic Engineering 14:149-158.

YOSHIZAWA, T., OHTSUKA, Y., OKAMOTO, Y., SHINOTO, A., and KIMOTO, K. 1987. Automatic three dimensional measurement by the projection of a grating pattern. In: Stokes, I., *et al.*, eds. Surface Topography and Spinal Deformity. New York: Fischer Verla. 403-411.